Theory of energy-transfer collisions of excited sodium atoms: $3P+3P \rightarrow 3S+5S$ or $4D$

S. Geltman
Joint Institute for Laboratory Astrophysics, University of Colorado and National Institute of Standards and Technology, Boulder, Colorado 80309-0440
(Received 21 February 1989)

The energy transfer between a pair of excited Na($3p$) atoms leading to Na($3s$)+Na($5s$) and Na($3s$)+Na($4d$) final states is studied in a semiclassical coupled-state theory. Classical trajectories are evaluated from the average adiabatic potentials of previously calculated excited molecular states of Na_2. With this specification of average nuclear $\mathbf{R}(t)$ for atoms approaching in a given magnetic quantum number (m_a,m_b) substate, we solve the coupled equations for the time-dependent Schrödinger equation in the 21-state diabatic basis set (including $3p$, $3s$, $5s$, and $4d$) of atom pairs. The coupling terms arise from the dipole-dipole interaction. Excellent agreement is obtained with the data of the two most recent measurements of the $3s+4d$ and $3s+5s$ energy-transfer cross sections at $T\sim 500$–600 K. Extension to low temperature shows a rising $3s+5s$ cross section as a result of a net attractive adiabatic potential in the $(m_a,m_b)=(1,0)$ incident channel, as also occurs for associative ionization.

I. INTRODUCTION

Over the last 15 years there has been a large effort invested in studying the processes that occur in a dense sodium vapor when it is excited with laser radiation at the $3s$-$3p$ resonance wavelength.[1] Collisions of two Na($3p$) atoms may lead to a variety of final states, including $Na_2^+ + e$ for associative ionization, or Na(nl) +Na($n'l$) for energy transfer. Associative ionization has been studied experimentally most recently by Bonanno *et al.*[2] and Huennekens and Gallagher,[3] and theoretically by Geltman.[4] The energy-transfer processes, which are most favored by electronic energy balance with the initial states, have final states nl and nl' of $3s+5s$ (E_f-$E_i=-735$ cm^{-1}), $3s+4d$ (E_f-$E_i=613$ cm^{-1}), and $3s+4f$ (E_f-$E_i=653$ cm^{-1}). Measurements of the rate coefficients and derived cross sections have been carried out for one or more of these processes by a number of groups.[5–10] The only theoretical work on these processes has been done by Kowalczyk[11] on $3s+4d$ and by Allegrini *et al.*[10] on $3s+4d$ and $3s+4f$ energy transfer.

There is considerable disagreement among many of the measured cross sections, except for the measurements of Huennekens and Gallagher[8] and Allegrini *et al.*[9] on $3s+5s$ and $3s+4d$, which agree within their estimated errors. Kowalczyk's calculated result[11] for $3s+4d$ lies about a factor of 10 below these mutually consistent measured values, while the Allegrini *et al.*[10] calculation is a factor of 2–3 below. The Allegrini *et al.*[10] calculation for $3s+4f$ is consistent with their own measurement of that cross section.

The theoretical treatments to date have used apparent curve crossings at the rather large internuclear distances of $R \gtrsim 25a_0$, together with the Landau-Zener approximation for the transition probabilities. In the present work we apply an alternate formulation of the problem to the processes

$$\mathrm{Na}(3p)+\mathrm{Na}(3p)\rightarrow \mathrm{Na}(3s)+\mathrm{Na}(5s,4d)\ . \tag{1}$$

We find that diabatic curve crossings in the region of $5<R<14a_0$ are most important, and transition probabilities are evaluated from a full solution of the coupled-state Schrödinger equation.

II. GENERAL OUTLINE OF THEORY

We seek to treat the collision of two Na($3p$) atoms in the most general way possible within the limits of a semiclassical calculation. This means that the transitions among the electronic states of the atoms are consequences of the excited atoms following a prescribed classical trajectory $\mathbf{R}(t)$. Once this classical trajectory is assigned to a pair of initial Na($3p$) atoms in given magnetic quantum number m substates, one can, in principle, solve the time-dependent Schrödinger equation to get the probabilities for transitions to all final states which are energetically and dynamically accessible.

This procedure is, of course, an approximation since the nuclear and electronic motion are in reality, coupled and interdependent. A full quantum formulation would require an expansion of the form

$$\Psi(\mathbf{r},\mathbf{R})=\sum_i F_i(\mathbf{R})\psi_i(\mathbf{r})\ ,$$

or

$$\Psi(\mathbf{r},\mathbf{R})=\sum_j G_j(\mathbf{R})\phi_j(\mathbf{r};\mathbf{R})\ , \tag{2}$$

where the electronic states may or may not depend parametrically on the internuclear separation, i.e., one may use atomic or molecular basis states. To represent associative ionization a molecular basis set should be used, and the G_j's would have to include states of nuclear motion representing vibration in Na_2^+. The solution of the corresponding time-independent Schrödinger equa-

tion subject to scattering boundary conditions would be a formidable computational project, so we seek semiclassical simplifications.

Our present treatment will involve two distinct phases. The first is the selection of classical trajectories. This is based on detailed adiabatic potential curves which have been evaluated by other workers for pairs of excited Na atoms which dissociate to the $3p+3p$ limit, and is covered in Sec. III. The second phase concerns the solution of the time-dependent Schrödinger equation for a pair of atoms which experience a mutual interaction while traversing that trajectory. That will be covered in Sec. IV, and the results will be compared with the experiment and discussed in Sec V.

III. INITIAL ADIABATIC STATES AND TRAJECTORIES

Adiabatic energies for an atom pair at separation R are the fully diagonalized values for the total electronic Hamiltonian. The locus of these levels as a function of R form the adiabatic energy curves, and they will asymptotically go to the appropriate separated-atom values. They do not depend on the direction of $\mathbf{R}$ in the laboratory system since the total energies are invariant with respect to rotation of the atoms. By use of the Born-Oppenheimer separation of electronic and nuclear motion, it follows that a single adiabatic energy curve will serve as the potential energy for the motion of the nuclei if there are no appreciable perturbations to alter the system's electronic state. This of course is the basis for evaluating vibrational structure in molecules in terms of adiabatic potential curves. In the case of collisions of excited atoms there is an appreciable probability for an electronic transition (as is seen in the following sections), so the choice of a particular classical path is a bit more questionable. However, since the *final* adiabatic potential curves are not very different from the initial ones, it appears that the nuclear motion will not be perturbed appreciably in mid trajectory as a result of electronic transitions.

The adiabatic potential-energy curves for pairs of Na atoms having Σ, Π, and Δ character and arising from dissociated states up to $3p+3p$ have been evaluated by Henriet and Masnou-Seeuws.[12] Those dissociating to $3p+3p$ may be associated as follows with the atomic m_a and m_b (m_a,m_b) magnetic quantum numbers of the separated atoms:

$$(m_a=1,\ m_b=1)\rightarrow {}^1\Delta_g,\ \text{or}\ {}^3\Delta_u\ ;$$

$$(m_a=1,\ m_b=0)\rightarrow {}^1\Pi_g,\ {}^3\Pi_g,\ {}^1\Pi_u,\ \text{or}\ {}^3\Pi_u\ ;$$

$$(m_a=0,\ m_b=0)\rightarrow {}^1\Sigma_g^+,\ \text{or}\ {}^3\Sigma_u^+\ ;$$

$$(m_a=1,\ m_b=-1)\rightarrow {}^1\Sigma_u^-,\ {}^3\Sigma_u^+,\ {}^1\Sigma_g^+,\ \text{or}\ {}^3\Sigma_g^-\ .$$

All the other of the nine (m_a,m_b) combinations are asymptotically degenerate with one of the above independent cases. For example, $(m_a,m_b)=(-1,-1)$ is asymptotically degenerate with (1,1), and $(m_a,m_b)=(0,-1)$ is asymptotically degenerate with (1,0), etc. Since the atoms are identical, the choice of which is atom A and which is atom B is arbitrary.

Each of the above four (m_a,m_b) combinations defines an independent incident channel for the energy-transfer process. Atoms approaching one another in any one such incident channel will be in the above corresponding adiabatic molecular states with probabilities determined by statistical weights. We may thus construct the average potentials in terms of the adiabatic potentials of Henriet and Masnou-Seeuws,

$$\begin{aligned}
\bar{V}(1,1)&=\tfrac{1}{4}[V({}^1\Delta_g)+3V({}^3\Delta_u)]\ ,\\
\bar{V}(1,0)&=\tfrac{1}{8}[V({}^1\Pi_g)+3V({}^3\Pi_g)+V({}^1\Pi_u)+3V({}^3\Pi_u)]\ ,\\
\bar{V}(0,0)&=\tfrac{1}{4}[V({}^1\Sigma_g^+)+3V({}^3\Sigma_u^+)]\ ,\\
\bar{V}(1,-1)&=\tfrac{1}{8}[V({}^1\Sigma_u^-)+3V({}^3\Sigma_u^+)+V({}^1\Sigma_g^+)+3V({}^3\Sigma_g^-)]\ .
\end{aligned}\tag{3}$$

At very large R these go into the asymptotic form $c_5/R^5+c_6/R^6$. Here c_5/R^5 is the first-order diagonal matrix element of the quadrupole-quadrupole interaction term between two Na($3p$) atoms. This is the lowest-order term in the multipole expansion for the interaction which is nonvanishing, as diagonal first-order matrix elements of the dipole moments will vanish. The c_6/R^6 van der Waals interaction is the diagonal matrix element in second order of the dipole-dipole interaction term.

We have evaluated c_5 and c_6 for each of the incident (m_a,m_b) channels using the Bates-Damgaard method[13] for the atomic dipole and quadrupole radial matrix elements, and these are given in Table I. Since the adiabatic potentials of Henriet and Masnou-Seeuws have been evaluated out to $R=16a_0$, we have smoothly joined their results to the asymptotic values at $R\geq 24a_0$. The resulting average adiabatic potentials are given in Fig. 1.

These potentials are used to describe the average trajectory for a pair of Na($3p$) atoms which enter a collision in the (m_a,m_b) channel. An example of the resulting orbits for the (1,0) incident channel at a relative velocity of 1.2×10^5 cm/s is given in Fig. 2. For the lower values of impact parameter, the distance of closest approach will be $\sim 5a_0$, corresponding to the turning points due to the repulsive part of the potential $\bar{V}(1,0)$, as seen in Fig. 1. At large enough impact parameter the orbit will no longer penetrate and approach a rectilinear path.

As we will see in Sec. IV, the radial range for the diabatic curve crossings which lead to electronic transitions is $5<R<14a_0$. From the orbits in Fig. 2 we can expect this range to be reached at this velocity by impact parameters $\rho\lesssim 23a_0$. Since the average potentials in Fig. 1 are qualitatively similar to one another, one can expect qualitatively similar sets of orbits to result for all (m_a,m_b) cases. The repulsive hill in $\bar{V}(0,0)$ at $R\cong 15a_0$ results in

TABLE I. Asymptotic parameters for the Na($3p$)+Na($3p$) interaction.

m_a	m_b	c_5 (a.u.)	c_6 (a.u.)
1	1	365.4	−6303.0
1	0	−730.8	−9134.0
0	0	1462.0	−147.0
1	−1	365.4	−7550.0

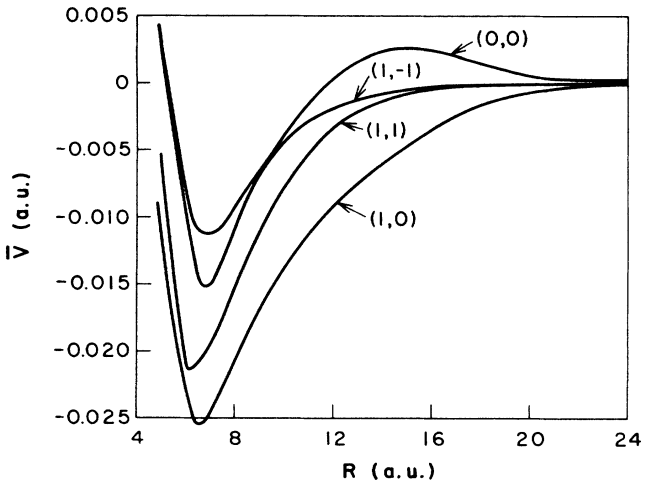

FIG. 1. Average adiabatic potentials $\bar{V}(m_a,m_b)$ for indicated (m_a,m_b) values.

nonpenetrating orbits for $v \lesssim 1\times10^5$ cm/s, and hence very low transition probabilities for lower velocities. Similarly, the much smaller potential hills in the (1,1) and (1,−1) channels (due to $c_5>0$) will give effective cutoffs in their respective transition cross sections at much lower velocities. The only channel that is effectively open at all velocities is (1,0) since its $c_5<0$. In fact, at ultralow velocities (for example, $T\sim1$ mK, which are attainable by laser atom-cooling techniques[14]) there is a large focusing of atoms in that channel from very large impact parameters ($\sim250a_0$) to inwardly spiraling orbits.[4] This is similar to the Langevin orbiting in an ion-atom collision, where the effective potential is the $-\alpha/R^4$ polarization attraction.

IV. DIABATIC BASIS STATES AND TRANSITIONS

Having adopted the average trajectory that is expected to be followed in a collision of a pair of Na(3p) in the

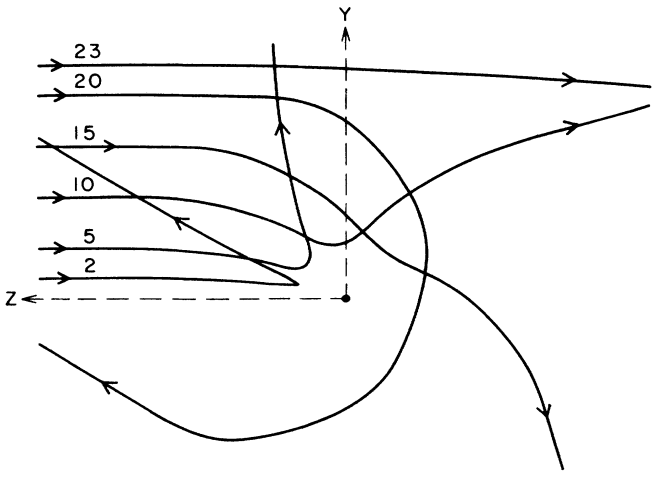

FIG. 2. Typical orbits for collisions on potential $\bar{V}(1,0)$ at $v=1.2\times10^5$ cm/s for various impact parameters.

(m_a,m_b) substates, we must now adopt a basis set of diabatic states to describe the dynamics of transitions. Any complete set may be used for this, but some are more convenient than others. For example, the adiabatic states discussed in Sec. III are an acceptable basis set, but they are complicated, correlated molecular wave functions, and only a small part of the total number required for the transition to $3s+4d$ have been evaluated by Henriet and Masnou-Seeuws.[12] Furthermore, since they diagonalize the full electronic Hamiltonian at each R, the perturbation that would induce transitions between electronic states is the coupling between electronic and nuclear motions, $\sim(d\mathbf{R}/dt)\cdot\nabla_{\mathbf{R}}\phi_j(\mathbf{r};\mathbf{R})$. This is a small perturbation for the thermal velocities of interest.

Instead, we will adopt the diabatic basis set that is simplest to handle, and that is the set of separated-atom wave functions defined in the laboratory system, or

$$\psi_i(\mathbf{r}_a,\mathbf{r}_b)=|n_a l_a m_a, n_b l_b m_b\rangle \ . \tag{4}$$

We neglect fine-structure effects, which will be small except at very low velocities or temperatures (the $3^2P_{1/2,3/2}$ splitting equals kT at about $T\cong25$ K). Expanding the full time-dependent electronic wave function as

$$\Psi(\mathbf{r},t)=\sum_i a_i(t)\psi_i(\mathbf{r}_a,\mathbf{r}_b)\exp\left[-i\int^t dt H_{ii}\right] , \tag{5}$$

the Schrödinger equation is converted into the set of coupled equations for the transition amplitudes,

$$\dot{a}_j=-i\sum_i{}' H_{ji}a_i\exp\left[i\int^t dt(H_{jj}-H_{ii})\right] . \tag{6}$$

(Atomic units are used throughout unless otherwise specified.) Here H_{ij} is the matrix of the full electronic Hamiltonian $H=H_0+H'$ taken with respect to the basis states (4),

$$H_{ij}=E_i\delta_{ij}+H'_{ij} \ , \tag{7}$$

where H' is the interaction potential between the two atoms, and the infinitely separated atoms are described by

$$H_0\psi_i=E_i\psi_i \ . \tag{8}$$

The lower limit on $\int^t dt$ in (6) is arbitrary as it merely affects the phase factor.

The diagonal elements $H_{ii}(R)$ are the *diabatic* energy curves. It should be noted that they are not unique but depend entirely on the basis set chosen. This differs from the adiabatic curves, which are unique in principle in that they are defined ideally as the electronic eigenvalues at separation R. In practice, even the adiabatic curves are not unique in that they are approximated by diagonalized energies in some subspace of a molecular basis set. This latter property prevents the crossing of adiabatic states of a given molecular symmetry. Diabatic states of a given symmetry are, of course, free to cross one another, and indeed it is these crossings that give rise to the main flow of amplitude among the basis states.

We describe the interaction potential in terms of the multipole expansion for the interaction of two electronic charge clouds (neutral systems[15])

$$H' = 16\pi^2 \sum_{\alpha,\beta} (-1)^{\beta} [4\pi(2\alpha+1)(2\beta+1)(2\alpha+2\beta+1)]^{-1/2} \frac{r_a^{\alpha} r_b^{\beta}}{R^{\alpha+\beta+1}} \times \sum_{\lambda,\mu} \left[\frac{(\alpha+\beta-\lambda-\mu)!(\alpha+\beta+\lambda+\mu)!}{(\alpha-\lambda)!(\alpha+\lambda)!(\beta-\mu)!(\beta+\mu)!} \right]^{1/2} Y_{\alpha,\lambda}(\hat{\mathbf{r}}_a) Y_{\beta,\mu}(\hat{\mathbf{r}}_b) Y^*_{\alpha+\beta,\lambda+\mu}(\hat{\mathbf{R}}) \ . \quad (9)$$

We choose our laboratory system such that the $+Z$ axis is along $-\mathbf{v}$ ($\mathbf{v}$ is the relative velocity vector for atom A incident on atom B), and the YZ plane is the collision plane.

Consider the minimum subset of basis states needed to describe the transitions

$$\mathrm{Na}(3p\ m_a) + \mathrm{Na}(3p\ m_b) \rightarrow \mathrm{Na}(3s) + \mathrm{Na}(5s) \rightarrow \mathrm{Na}(3s) + \mathrm{Na}(4d\ m) \ , \quad (10)$$

that is,

$$|n_a l_a m_a, n_b l_b m_b\rangle = |3\,1\,m_a, |3\,1\,m_b\rangle \ , = |3\,0\,0, 5\,0\,0\rangle \ , = |3\,0\,0, 4\,2\,m\rangle \ . \quad (11)$$

We would first like to examine the diagonal diabatic curves in this subspace. The only term in (9) contributing to a diagonal matrix element which is asymptotic to $3p+3p$ is the $\alpha=\beta=2$ quadrupole-quadrupole term, or

$$\langle 3\,1\,m_a,\ 3\,1\,m_b | H | 3\,1\,m_a,\ 3\,1\,m_b \rangle = E_{3p,3p} + \frac{c_5(m_a m_b)}{R^5} P_4(\cos\theta) \quad (12)$$

where $\cos\theta = \hat{\mathbf{k}}\cdot\hat{\mathbf{R}}$. All other terms in (9) give a vanishing contribution because of the parity or triangular selection rules. It is this term, which also gives rise to the adiabatic asymptotic interaction c_5/R^5, that was discussed in Sec. III. Since the adiabatic potential is evaluated with respect to a rotating coordinate system, the $P_4(\cos\theta)$ above would go to 1 (since $\theta \rightarrow 0$ in that system).

A similar examination of the diagonal diabatic curves which are asymptotic to $3s+5s$ and $3s+4d$ shows that there are *no* terms in expansion (9) that contribute nonvanishingly. This is a consequence of the general selection rule that $s \rightarrow s$ transitions are strictly forbidden via all multipole moments. Thus the two final diagonal diabatic curves in our present representation are constants and all crossings will be determined by the R,θ dependence of Eq. (12) on the appropriate classical orbit.

In Fig. 3 we show the radial dependence of these diabatic curves. The coefficient $P_4(\cos\theta)$ will introduce a number of crossings with the constant final-state curves. This will mean that probability will flow strongly among the basis states near the crossings during a collision. It confirms that we are in a strong-coupling regime where a full solution of the coupled equations (6) is necessary. We point out that the multipole expansion (9) is valid only when the atoms are well separated so that there is little actual overlap of the charge clouds. When the overlap is appreciable this expansion loses its validity. Stated mathematically, (9) is an asymptotic expansion, which is not absolutely convergent at each R. It is thus not valid to allow the R^{-5} form in (12) to continue indefinitely to small R. To take account of this we have cut off the R^{-5} form at a value of R which is smaller than all of the "radial crossings" in Fig. 3. We have chosen $R_{CO} = 8a_0$, and replace R^{-5} in (12) by R_{CO}^{-5} for $R < R_{CO}$. This approximation in practice only affects the region $5 < R < 8a_0$ since our classical orbits do not penetrate to $R < 5$ anyway. In this region the factor $\exp[i\int^t dt\,(H_{jj} - H_{ii})]$ in (6) oscillates so rapidly as to not affect transition probabilities appreciably.

The effect of the $P_4(\cos\theta)$ factor in (12) will be to cause more oscillations of the initial diabatic curve between the two final constant diabatic states, since P_4 has four zeros in $\pi > \theta > 0$, and the orbits sweep through a large range of θ as seen in Fig. 2. The sign changes in $P_4(\cos\theta)$ will cause crossings of the initial diabatic curve with *both* final diabatic states, no matter what the sign of c_5 (m_a, m_b) is. These are shown in Fig. 4 for the (1,0) channel where the initial diabatic curve is plotted as a function of time along the trajectory for various impact parameters.

We have given some consideration to the application of the Landau-Zener approximation[16] to transitions at these crossings. The Landau-Zener parameter at crossing time t_c is

$$q = 2\pi \frac{[H_{12}(t_c)]^2}{\left| \frac{d(H_{11} - H_{22})}{dt} \right|_{t_c}} \ , \quad (13)$$

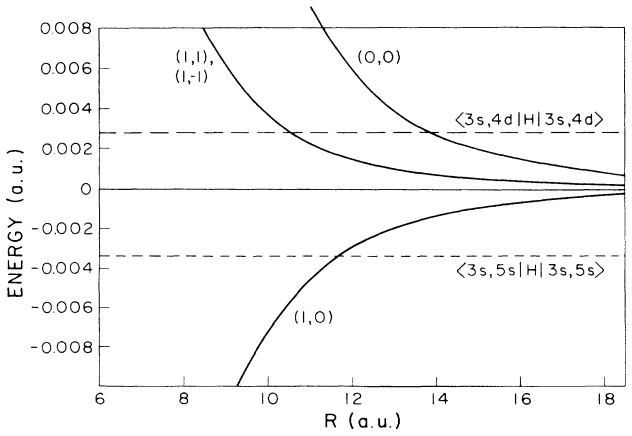

FIG. 3. Radial dependence of the diagonal diabatic matrix elements of the electronic Hamiltonian,

$$\langle 3p\ m_a, 3p\ m_b | H | 3p\ m_a, 3p\ m_b \rangle = E_{3p,3p} + c_5(m_a, m_b)/R^5 \ ;$$

values of (m_a, m_b) indicated (zero taken at $E_{3p,3p}$).

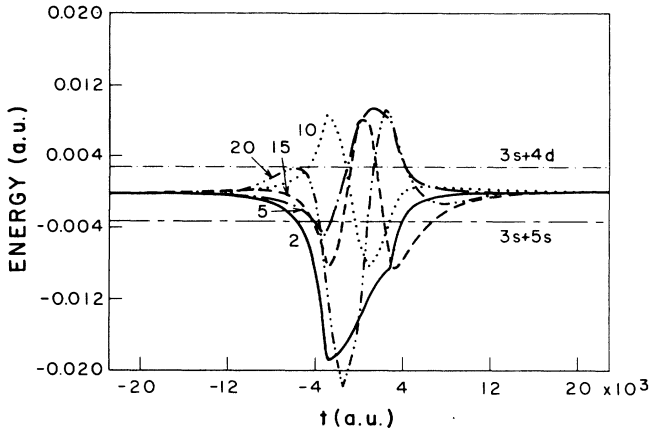

FIG. 4. Time dependence of $\langle 3p\,1,3p\,0|H|3p\,1,3p\,0\rangle$ along the trajectory prescribed by $\bar{V}(1,0)$ at $v=1.2\times10^5$ cm/s for various impact parameters. The zero of time is taken at the distance of closest approach, and crossings with the final diabatic $3s+5s$ and $3s+4d$ levels are shown.

and the corresponding transition probability at the crossing is

$$p=1-e^{-q}\ .$$

In general, this is a reasonable approximation if p is not too large, say if $q\lesssim1$ or $p\lesssim0.5$. We find that for many of the crossings encountered in this problem there are very large of values of q, say $q>10$, which indicates a strong-coupling situation ($p\cong1$), and hence a breakdown of the Landau-Zener approximation. Another deficiency of the Landau-Zener method in this case is its assumption that there is no coherence between crossings. The occurrence of closely successive crossings of $3s+5s$ and $3s+4d$ final states, as seen in Fig. 4, suggests that the phase relationships between them may be important. A third difficulty with the Landau-Zener approximation is that it is applicable only to the crossing of nondegenerate states. The high degeneracy of the $3s+4d$ final state makes its application to the present case inappropriate.

Total energy conservation, including both the nuclear and electronic degrees of freedom, is not automatically satisfied in a semiclassical treatment. The assignment of a classical orbit governed by a potential-energy curve, as we are presently doing, simply treats the nuclear translational energy as a constant throughout the collision. Actually, there is an interchange between nuclear and electronic energies in such a way as to preserve overall energy. This would be incorporated into the boundary conditions in a full time-independent quantum treatment based on expansion (2). This includes the conversion of initial translational energy into molecular vibrational energy, as occurs in the associative ionization process. The semiclassical time-dependent Schrödinger equation (6) does not insure overall energy conservation since an external perturbation is assumed to be present. This is the prescribed collision trajectory $\mathbf{R}(t)$ in the present case, or it could be an applied laser field where $H'\sim\mathbf{r}\cdot\mathbf{E}_0\cos(\omega t)$. In either case it is assumed that the source of the external perturbation is unaffected by the quantum transitions it is causing.

From Fig. 3 it is seen that the transition to $3s+5s$ is exothermic, i.e., has no threshold, while the transition to $3s+4d$ is endothermic by 613 cm^{-1}, which corresponds to a threshold velocity of 1.130×10^5 cm/s. In our adopted basis set there are nine (m_a,m_b) combinations and ten substates of $3s+4d$ m (each pair state must appear symmetrically on atom A and B). This means that there are 11 basis states below the $3s+4d$ threshold, and there are 21 basis states above this threshold which must be included in expansion (5).

The off-diagonal matrix element H'_{ij} is evaluated from the dipole-dipole term in (9) ($\alpha=\beta=1$), and thus will couple the initial state to either of the two final states, but will not connect the $3s+5s$ and $3s+4d$ final states. They are not directly coupled to each other by any term in (9), again because of the $s\not\to s$ selection rule. The H'_{ij} also depend on θ, since the dipole-dipole term in (9) has the more familiar form

$$V_{d\text{-}d}=\frac{1}{R^3}[\mathbf{r}_a\cdot\mathbf{r}_b-3(\mathbf{r}_a\cdot\hat{\mathbf{R}})(\mathbf{r}_b\cdot\hat{\mathbf{R}})]\ . \tag{14}$$

In terms of the polar angle θ of a trajectory point and Cartesian electron coordinates, this becomes

$$\frac{1}{R^3}[x_ax_b+(1-3\sin^2\theta)y_ay_b+(1-3\cos^2\theta)z_az_b$$
$$-3\sin\theta\cos\theta(y_az_b+z_ay_b)]\ ,$$

in terms of which the needed transition matrix elements are readily found. We use the Bates-Damgaard radial matrix elements, $(3p|r|3s)=4.223$, $(3p|r|5s)=-0.9182$, and $(3p|r|4d)=-1.658$. For consistency with our procedure with the diagonal matrix elements, we also apply the same cutoff to the radial R^{-3} dependence of the off-diagonal matrix element.

V. RESULTS AND DISCUSSION

We use the RKF solver[17] for the set of first-order linear equations (6). The 21 equations for complex a_j become 42 real equations. As the times needed for solutions of such large sets of equations on the VAX 8600 computer is considerable, we have lowered the relative error requirement and the number of impact parameters such that the resulting cross sections have a numerical accuracy of $\pm10\%$. An example of the variation of the transition probabilities P_{3s+5s} and P_{3s+4d} with impact parameter is shown in Fig. 5. It is seen that there are many oscillations, indicating a strong-coupling situation. Although the incident channel is a particular (m_a,m_b) combination, there is a redistribution among all the (m_a,m_b) states during the course of the collision. This is seen by examining the individual final $(3p\ m_a)+(3p\ m_b)$ probabilities. Note that the sudden drop in transition probabilities at $\rho\cong23$ is a result of the trajectories no longer penetrating into the crossing region of the diabatic curves.

The individual channel transition cross sections are

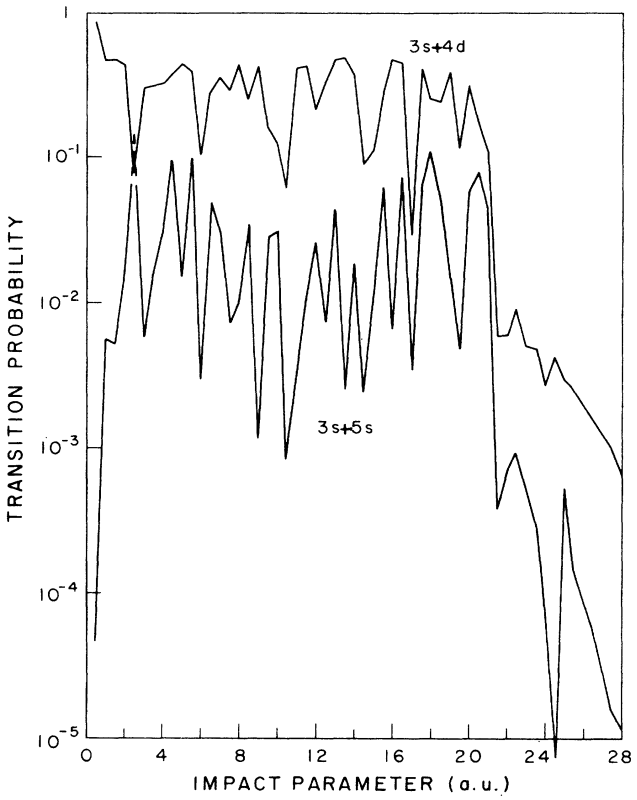

FIG. 5. Transition probability to the $3s+5s$ and $3s+4d$ final states at $v=1.2\times10^5$ cm/s and incident channel $(m_a,m_b)=(1,0)$ as a function of impact parameter.

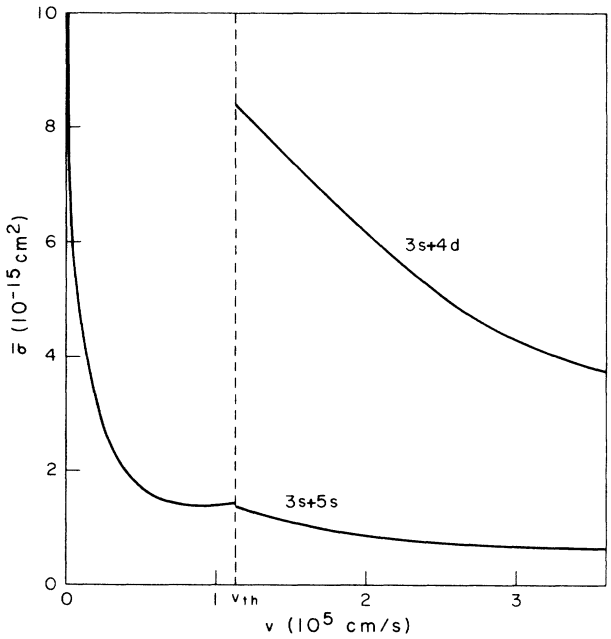

FIG. 6. Average transition cross section to the $3s+5s$ and $3s+4d$ final states as a function of initial relative velocity. The threshold velocity for the $3s+4d$ transition is 1.130×10^5 cm/s.

given in Table II. The statistically weighted average cross sections,

$$\bar{\sigma}=\tfrac{1}{9}[2\sigma(1,1)+4\sigma(1,0)+\sigma(0,0)+2\sigma(1,-1)] \quad (15)$$

are shown in Fig. 6. There is a discontinuity in $\bar{\sigma}_{3s+5s}$ at the threshold for $\bar{\sigma}_{3s+4d}$ since different basis sets are used below and above the threshold. It is fortuitous that the discontinuity in $\bar{\sigma}_{3s+5s}$ is small as it is, since the individual channel cross sections each have larger discontinuities, as can be seen in Table II. One would expect that exact cross sections from a full quantum treatment would be continuous at the $3s+4d$ threshold with a significant departure from the semiclassical values over a velocity range $\sim(m/M)^{1/2}v_{\rm th}$. This would also apply to $\bar{\sigma}_{3s+4d}$, which should go to zero at its threshold from phase-space considerations (Wigner threshold law). Note that $\bar{\sigma}_{3s+5s}$ rises indefinitely as $v\to0$ because of the attractive adiabatic potential in the (1,0) channel (see Tables I and II). As v decreases, larger and larger impact-parameter trajectories are pulled into the diabatic crossing region.

The thermally averaged cross sections are given in Fig. 7. The rising $3s+4d$ cross section reflects the increasing overlap with the Maxwell distribution. Since $\bar{\sigma}_{3s+4d}(v)$ is decreasing somewhat less rapidly than $1/v$, one expects this rise to continue until $T>2E_{\rm th}/k$, or up to $T\cong1800$ K. The slowly falling thermal $3s+5s$ cross section

TABLE II. Cross sections for specific incident channels (m_a,m_b) (in 10^{-15} cm^2).

		v (10^5 cm/s)					
m_a	m_b	0.1	0.5	1.0	1.2	2.4	3.6
				$3p+3p\to3s+5s$			
1	1	0.903	1.67	0.973	1.17	0.698	0.638
1	0	8.38	2.47	2.09	1.29	0.328	0.509
0	0	0.008	0.030	0.075	0.677	2.17	1.68
1	−1	2.66	1.10	1.18	1.78	0.943	0.490
				$3p+3p\to3s+4d$			
1	1				5.63	3.15	3.29
1	0				11.59	7.15	4.30
0	0				1.37	4.39	4.90
1	−1				7.30	4.09	2.58

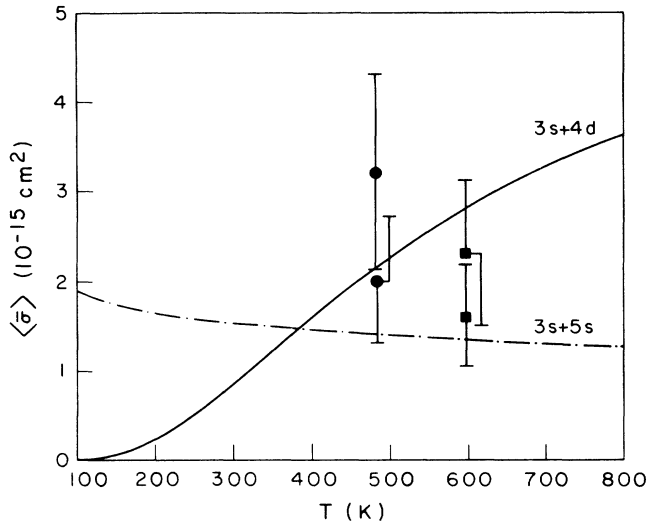

FIG. 7. Velocity-averaged (Maxwell distribution) transition cross sections to $3s+5s$ and $3s+4d$. The measured points are those of Huennekens and Gallagher (Ref. 8) at 597 K and Allegrini *et al.* (Ref. 9) at 483 K. The higher-lying experimental point is the $3s+4d$ cross section in both measurements.

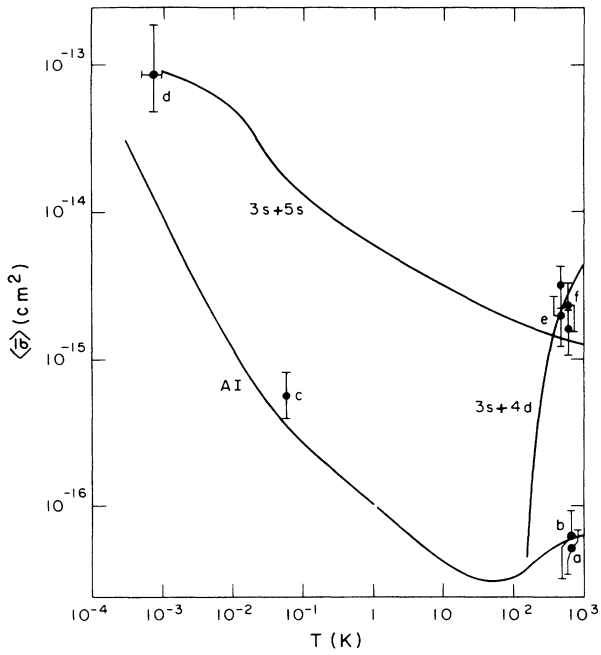

FIG. 8. Extended-range temperature variation of $3s+5s$ and $3s+4d$ average cross sections [values for $T<100$ K are taken as $\bar{\sigma}$ ($v=\sqrt{2kT/M}$)], compared with average cross section for associative ionization evaluated in Ref. 4, and measured values. For AI, *a*, Ref. 3; *b*, Ref. 2; *c*, Ref. 18; *d*, Ref. 14; for energy transfer, *e*, Ref. 9; and *f*, Ref. 8.

reflects the behavior of $\bar{\sigma}_{3s+5s}(v)$ in this temperature range. The results of Huennekens and Gallagher[8] and Allegrini *et al.*[9] are included in Fig. 7, and we see that there is excellent agreement with our present results. The three measurements[5–7] which are not included in Fig. 7 give cross sections that differ from these by one or more orders of magnitude. Both Huennekens and Gallagher[8] and Allegrini *et al.*[9] discuss possible experimental reasons for these widely differing results. A previous calculation[11] gives a value of $\bar{\sigma}_{3s+4d}=1.17\times10^{-15}$ cm^2 at $T=550$ K, which is about a factor of 2 lower than the present calculation. That calculation relied on a different set of basis states, which led to apparent crossings at much large separations ($R\simeq30a_0$) than we encounter here, and with the use of the Landau-Zener formula.

An extension of our present results down to ultralow temperatures is given in Fig. 8. As mentioned above, $\langle\bar{\sigma}_{3s+5s}\rangle$ for $T<1$ K comes entirely from the (1,0) channel. The $\langle\bar{\sigma}_{3s+5s}\rangle$ values in Fig. 8 for $T<10$ K are taken from $\bar{\sigma}_{3s+5s}(v)$ at $v=(2kT/M)^{1/2}$. For comparison, we show the previously calculated[4] and measured[2,3,14,18] associative-ionization (AI) cross sections. That theoretical curve followed from a semiclassical perturbation theory calculation on approximately the same adiabatic trajectories as are used presently. The fact that the AI cross section is substantially below the present energy-transfer cross sections is consistent with the applicability of perturbation theory for that case, as opposed to the necessity for a coupled-equation solution presently. The apparent shoulder on $\langle\bar{\sigma}_{3s+5s}\rangle$ at low T and its absence from $\langle\bar{\sigma}_{\rm AI}\rangle$ reflects the difference between the perturbative AI calculation and the coupled-equation solution for the $3s+5s$ transition. In the former at low T, $\sigma_{\rm AI}\cong\pi\rho_{\rm max}^2\bar{P}_{\rm AI}$, and the main T dependence comes from the $\bar{v}$ variation of the maximum capture impact parameter $\rho_{\rm max}$, with $\bar{P}_{\rm AI}$ remaining almost constant. In the latter, the full solution of the coupled equations along the trajectory is such that $\bar{P}_{3s+5s}$ has a stronger dependence on $\bar{v}$ than does $\bar{P}_{\rm AI}$, giving the cross sections somewhat different shapes as a function of T.

We have omitted from our basis set the possible final state $3s+4f$, which lies above the $3s+4d$ level by only 40 cm^{-1}. It is clear from Fig. 4 that almost all crossings with the $3s+4d$ level will also involve one with the $3s+4f$ level. However the off-diagonal coupling between $(3p\,m_a)+(3p\,m_b)$ and $3s+4f$ will involve the dipole-quadrupole term [$\alpha=1,\beta=2$ and $\alpha=2,\beta=1$ in (9)] varying as R^{-4}. This would mean a weaker coupling at the crossing than for the dipole-dipole transitions. The energy transfer cross section to $3s+4f$ has been also measured by Allegrini *et al.*[10] at $T=523$ K with the result of $(5.7\pm2.3)\times10^{-16}$ cm^2. This is a factor of 3–6 lower than the $3s+5s$ ($4d$) cross sections, which helps to justify the omission of that state from our set of basis states. It should be noted that Davidson *et al.*[19] find a transfer cross section to $3s+4f$ which is only about a factor of 2 below the $3s+4d$ value. However, the inclusion of $3s+4f$ basis states would have meant an increase in the number of real coupled equations from 42 to 70, making the calculation prohibitive. Huennekens and Gallagher[8] also reported estimated cross sections to the more remote $3s+6s$ and $3s+5d$ endothermic final states which lie below the $3s+4d$ cross section by the factors 10^{-2} and 3×10^{-3}, respectively.

Since the fine-structure splitting of $3\,^2P_{1/2,3/2}$ is 17.2 cm^{-1} ($\cong kT$ at $T \cong 25$ K), it is clear that care must be taken in comparing the results of measurements at ultralow temperatures with the present results. For example, if the Na atoms are cooled by pumping to a particular JFM_F state, it is legitimate to ask how subsequent energy-transfer cross sections are to be compared with our present $\langle \bar{\sigma} \rangle$. Our present treatment of the dynamics of these processes indicates that the introduction of a spin-orbit interaction would be a negligible perturbation. For example, such an interaction is negligible compared with H'_{ij} at a crossing ($\sim 10^{-3}$ a.u.), and it would produce negligible shifts in the diabatic energies of Figs. 3 and 4. Thus apart from questions of the recoupling of angular momenta, the only real effect of fine structure on these processes is in the initial-state population mechanism. If the m_l states are not populated equally, one must do the appropriate Clebsh-Gordan algebra to combine our $\sigma(m_a, m_b)$ values in such a way that they represent the actual distribution of (m_a, m_b) states excited, while summing over all the other dynamically unimportant quantum numbers (JFM_F).

Another potentially more serious question which enters at ultralow temperatures is the fact that the radiative lifetime of Na($3p$) (~ 16 ns) becomes comparable or smaller than average collision times. A basic assumption in the present calculation is that the colliding excited sodium atoms are not coupled to the radiation field, and can lose their excitation energy only through collision channels. It would seem that AI and energy-transfer measured rates must be *lower* than theoretical rates which neglect the occurrence of radiative decays. This would account for the loss of transition probability when the atoms are on a collision trajectory but decay before the critical crossing region is reached. For example, the time for a pair of excited atoms at zero initial velocity to traverse the present trajectory from $R \cong 300a_0$ to the curve-crossing region is ~ 18 ns, which would amount to a decay survival probability of ~ 0.3. This question deserves more detailed separate attention, along with the question of quantum effects replacing classical trajectories at very low velocities.

In summary, we have treated the energy-transfer process of thermal collisions of excited Na($3p$) atoms to the $3s+5s$ and $3s+4d$ states. We have used a semiclassical method with realistic atomic trajectories based on known adiabatic potential curves. The transition probabilities were evaluated by numerical solution of the Schrödinger equation within the subspace of the $(3p\ m_a)+(3p\ m_b)$ and $3s+5s, 3s+(4d\ m)$ atomic basis states, subject to the perturbation resulting from the dipole-dipole interaction. The results are in excellent agreement with the two most recent measurements of these cross sections. The main processes omitted from the present basis set, associative ionization and energy transfer to $3s+4f$, are shown by other experimental and theoretical work to occur with much lower probability than the presently considered processes. We now feel that a good theoretical understanding of the mechanisms for these processes exists, and hope that these methods may be promising for other thermal energy-transfer processes.

ACKNOWLEDGMENTS

I am indebted to M. Allegrini, D. Pritchard, and J. Weiner for helpful discussions. I would also like to thank L. Kovalenko, C. Kunasz, X. P. Lu, S. V. ONeil, and G. Schatz for advice and help with computational problems. Partial support was provided by the National Science Foundation through Grant No. PHY86-04504, and all computations were done on the JILA VAX 8600 computer.

[1]For early reviews, see T. B. Lucatorto and T. J. McIlrath, Appl. Opt. **19**, 3948 (1980); A. Kopystynska and L. Moi, Phys. Rep. **92**, 135 (1982).

[2]R. Bonanno, J. Boulmer, and J. Weiner, Phys. Rev. A **28**, 604 (1983); Comments At. Mol. Phys. **16**, 109 (1985).

[3]J. Huennekens and A. Gallagher, Phys. Rev. A **28**, 1276 (1983).

[4]S. Geltman, J. Phys. B **21**, L735 (1988); **22**, 2049 (1989).

[5]D. J. Krebs and L. D. Shearer, J. Chem. Phys. **75**, 3340 (1981).

[6]V. S. Kushawaha and J. J. Leventhal, Phys. Rev. A **25**, 570 (1982).

[7]J. L. Le Gouët, J. L. Picqué, F. Wuilleumier, J. M. Bizeau, P. Dhez, P. Kock, and D. L. Ederer, Phys. Rev. Lett. **48**, 600 (1982).

[8]J. Huennekens and A. Gallagher, Phys. Rev. A **27**, 771 (1983).

[9]M. Allegrini, P. Bicchi, and L. Moi, Phys. Rev. A **28**, 1338 (1983).

[10]M. Allegrini, C. Gabbanini, L. Moi, and R. Colle, Phys. Rev. A **32**, 2068 (1985).

[11]P. Kowalczyk, Chem. Phys. Lett. **68**, 203 (1979); J. Phys. B **17**, 817 (1984).

[12]A. Henriet and F. Masnou-Seeuws, J. Phys. B **20**, 671 (1987).

[13]D. R. Bates and A. Damgaard, Philos. Trans. R. Soc. A **242**, 101 (1949).

[14]P. L. Gould, P. D. Lett. P. S. Julienne, W. D. Philips, H. R. Thorsheim, and J. Weiner, Phys. Rev. Lett. **60**, 788 (1988).

[15]H. Margenau and N. R. Kestner, *The Theory of Intermolecular Forces*, 1st ed. (Pergamon, London, 1969), p. 19.

[16]See, for example, S. Geltman, *Topics in Atomic Collision Theory* (Academic, New York, 1969), Chap. 27.

[17]The *RKF* subroutine is a coupled first-order differential equation solver using the Fehlberg fourth–fifth-order Runge-Kutta Method, written by H. A. Watts and L. F. Shampine. See G. E. Forsythe, M. A. Malcolm, and C. B. Moler, *Computer Methods for Mathematical Computation* (Prentice-Hall, Englewood Cliffs, NJ, 1977), Chap. 6.

[18]H. R. Thorsheim, Y. Wang, and J. Weiner, J. Opt. Soc. Am. B (to be published).

[19]S. A. Davidson, J. F. Kelly, and A. Gallagher, Phys. Rev. A **33**, 3756 (1986).